ELSEVIER

Optics and Lasers in Engineering 39 (2003) 293–304

OPTICS and LASERS in ENGINEERING

Homoclinic chaos in a laser: synchronization and its implications in biological systems

F.T. Arecchi[a,b,*], R. Meucci[a], A. Di Garbo[a,c], E. Allaria[a]

[a] *Istituto Nazionale di Ottica Applicata, Largo E. Fermi 6, 50125 Florence, Italy*
[b] *Departement of Physics, University of Firenze, Florence, Italy*
[c] *Istituto di Biofisica CNR, Via Alfieri 1, Ghezzano, Pisa, Italy*

Received 6 March 2001; accepted 12 April 2001

Abstract

Phase synchronization of a CO_2 laser with feedback, exhibiting homoclinic chaos, is realized by a tiny periodic perturbation of a control parameter. The deviations of the modulation frequency from the optimal one induce phase slips, thus yielding an imperfect phase synchronization. Based on the information of these phase slips, the modulation frequency can be readjusted until the phase slips are eliminated. In this way, a control loop which detects the phase slips provides an adaptive tracking of the natural frequency of the dynamical system. Moreover, we have shown that the system's susceptibility is largest when a periodic impulsive perturbation is applied near the saddle focus.

1. Introduction

It is known that the Poincaré map, i.e. the transformation which maps the intersection on a Poincaré section to the subsequent one, can be used to determine the stability of a periodic solution. Studying the stability of these intersection points and its bifurcations provide a local route to chaos [1,2]. The local bifurcations leading to chaos are known as period-doubling cascade, quasi-periodicity and intermittency. A local bifurcation should be contrasted with a global bifurcation which cannot be detected by analyzing small neighborhoods of unstable fixed points or cycles.

*Corresponding author. Istituto Nazionale di Ottica Applicata, Largo E. Fermi 6, 50125 Florence, Italy.

E-mail address: arecchi@ino.it (F.T. Arecchi).

0143-8166/03/$ - see front matter © 2002 Published by Elsevier Science Ltd.
PII: S0143-8166(01)00124-5

In this work, we are dealing with the case of homoclinic chaos which emerges from a global bifurcation.

An important homoclinic situation has been analyzed by Shilnikov and the resulting behavior is called Shilnikov chaos [3,4]. This situation occurs in three-dimensional state space when a saddle point has one real positive characteristic value γ and a pair of complex conjugate characteristic values—$\alpha \pm i\beta$. In this case, the saddle point is said to be a saddle focus. The saddle focus P has a one-dimensional unstable manifold and spiral behavior on a two-dimensional stable manifold.

Shilnikov showed that if there exists a homoclinic orbit to the saddle focus (i.e. there exists an orbit leaving the saddle focus along its unstable manifold which comes back to the saddle focus, in other words, the unstable manifold of P lies on the stable manifold of P; points on the homoclinic orbits approach the saddle focus for both $t \to \infty$ and $t \to -\infty$) and if $\gamma > |\alpha|$, then chaotic behavior occurs in a parameter range around the value at which the homoclinic orbit forms. This means that there exists a countable infinity of unstable periodic orbits in a neighborhood of the homoclinic orbit.

Homoclinic chaos of the Shilnikov type, initially observed in chemical [5] and laser experiments [6–8], shows striking similarities with the electrical spike trains traveling on the axons of animal neurons [9–14]. More generally, chemical oscillators based on an activator–inhibitor competition, which rule biological clocks controlling living rhythms, such as the heart pacemaker, hormone production, metabolism, etc. (Table 1), are subject to frequency fluctuations of homoclinic type, since in general, they cannot be reduced to a two-dimensional dynamics, as done in artificial clocks in order to have stable limit cycles [9–14].

The geometry of homoclinic chaos consists of regular orbits in phase space, which repeat themselves with a very small spatial variance. This regularity makes it difficult to extract relevant chaotic indicators from the geometry of the measured time series. Time wise however, the return period of these orbits is widely fluctuating, with very

Table 1
A list of the main biological rhythms, classified according to increasing period

Rhythm	Period
Neural rhythms[a]	0.01–10 s (and more?)
Cardiac rhythm[a]	1 s
Calcium oscillations[a]	1 s to several minutes
Biochemical oscillations[a]	1–20 min
Mitotic cycle[a]	10 min to 24 h (or more)
Hormonal rhythms[a]	10 min to several hours (also 24 h)
Circadian rhythms[a]	24 h
Ovarian cycle	28 d (human)
Annual rhythms	1 yr
Epidemiology and ecological oscillations	Years

[a] Rhythms occur at the cellular level (sometimes they may also arise from interactions between cells, e.g. in neural networks) (from Ref. [10]).

weak correlation between two successive returns. Being this the most apparent feature, it is convenient to characterize homoclinic chaos through the statistics of the return intervals [6–8]. The return map of successive return intervals consists of many branches which cross the fixed point line at a steep angle, so that successive iterations are sparse over the plane rather than clustered along the diagonal, as it should be for correlated sequences. Such a lack of correlation appears as a pseudo-Markovian behavior, even though it is purely deterministic. However, the highly unstable character of the return map makes the homoclinic chaos extremely vulnerable to noise [15], ruling out the hope of a practical way of controlling it.

On the other hand, the main concern in the dynamics of biological rhythms is to exploit the synchronization mechanisms, such as those which occur in large neuron assemblies during perceptual tasks, called "feature binding" [16,17] or those associated with an external periodic driving, such as the circadian rhythms [9–14]. Chaotic synchronization has been introduced as the identical behavior of two coupled chaotic systems [18], later extended to the case of only phase correlation of the two systems [19], or as the phase locking of a single chaotic system with respect to an external forcing [20]. In this latter case, extensive theoretical investigations of Rössler [21] and Lorenz models [22,23] have been provided. On the experimental side, chaotic synchronization has been exploited for communication with lasers [24] and its relevance demonstrated in some physiological phenomena (heartbeat [25], electrosensitive neurons [26]).

2. Synchronization of homoclinic chaos in a laser

A viable method of homoclinic synchronization is given in [27], showing its robustness notwithstanding the above mentioned fast decorrelation. We provide experimental evidence of such a synchronization on a laser operating in a homoclinic chaos regime by adding a small periodic modulation of a control parameter (Fig. 1).

The experiment has been performed on a single mode CO_2 laser with a feedback proportional to the output intensity. Precisely, a photon detector converts the laser output intensity in a voltage signal, which is fed back through an amplifier to an intracavity electro-optic modulator in order to control the amount of cavity losses. The average voltage on the modulator and the ripple around it are controlled by adjusting the bias and gain of the amplifier. We set these two control parameters so that the laser intensity displays a large spike above zero, followed by a fast damped train of a few oscillations and a successive longer train of chaotic oscillations of growing amplitude (Fig. 2). Damped and growing trains represent, respectively, the approach to, and the escape from, a saddle focus from where the trajectory rapidly returns to zero and then starts a new orbit. A suitable characterization of this regime can be provided by the return time of the main spike to a threshold level.

A digital oscilloscope records the laser output with a sampling time of 5 μs. From this time series we collect the times $\{t_j: j = 1, 2, \ldots, M\}$ at which the laser intensity crosses, with positive derivative, a threshold centered at 70% of the main peak. By using the set $\{t_j\}$ we define the average return interval as $T = 1/(M-1)\sum_{j=1}^{j=M-1} \times$

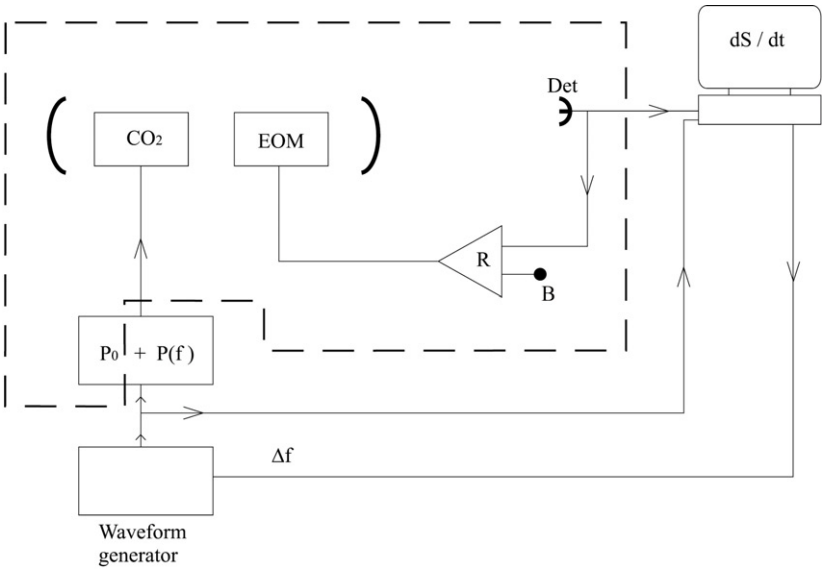

Fig. 1. Experimental setup. The region surrounded by a dashed line contour includes the setup for generating chaos, that is: (1) a single mode CO_2 laser excited by a power supply $P0$ and containing an intracavity electro-optic loss modulator; (2) the EOM driven by the voltage of a detector (Det) exposed to the laser intensity; the voltage passes through the amplifier R and is summed to a fixed bias voltage B. Applying to the pump a periodic modulation $P(f)$, the homoclinic spikes can be synchronized to the period $1/f$. As described in the text, the difference of periods between the laser and the waveform generator, averaged over a suitable time interval, provides the phase slip rate (dS/dt) which modifies the frequency of the clock.

$(t_{j+1} - t_j)$. This value, that is around 500 μs has been used to select an appropriate frequency range for the applied forcing. As for the control parameter to be modulated, we can choose either the bias voltage of the feedback amplifier or the pump of the gain medium. As our phenomena are relatively slow (around 2 kHz) we can safely modulate the discharge current of the laser tube, thus modifying the pump parameter from P_0 to $P_0(1 + m\sin(2\pi ft))$.

For a given modulation period T_{mod}, the phase locking states are characterized by evaluating the quantity $R = T/T_{\mathrm{mod}}$ for different values of the modulation amplitude. The existence of a $(p:q)$ phase locking state obviously implies that $R = p/q$. Different phase locking regimes have been reported in Fig. 3 together with the applied sinusoidal forcing. It is worth to note that the applied sinusoidal modulation does not strongly affect the dynamics close to the saddle focus. In other words, it is difficult to stabilize a periodic orbit visiting the neighborhood of the saddle focus. The main phase synchronization domain (1:1) is reported in Fig. 4(a) as a function of the amplitude V (expressed in units of mV or % of the d.c. value of the parameter to be modulated) and frequency v of the applied forcing. When the modulation frequency is close to the "natural frequency", that is, to the average frequency of the return intervals, the required modulation is below 1%. An increased modulation

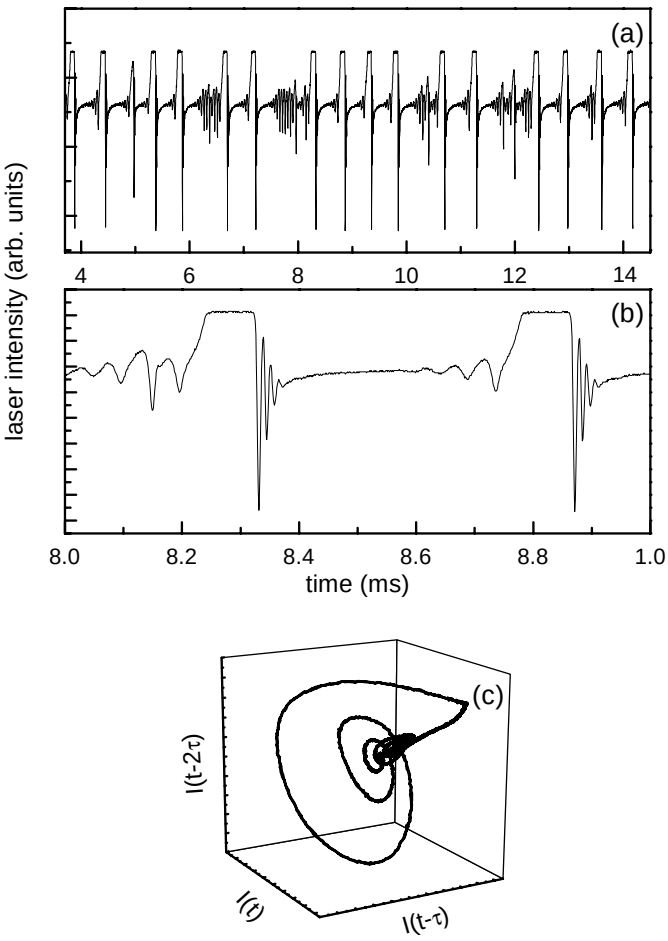

Fig. 2. (a) Experimental time series of the laser intensity for a CO_2 laser with feedback, in the regime of homoclinic chaos. (b) Time expansion of a single orbit. (c) Trajectory built by an embedding technique with appropriate delays.

amplitude up to 2% around the natural frequency provides a wide synchronization domain which attracts a frequency range of 30%. The criterion used to assign a point to the domain is that the R values be maintained for almost 10 periods. The behavior of R as a function of the forcing frequency is reported in Fig. 4(b) for two values of the modulation amplitude.

3. Phase slips and their control

The adopted criterion to define the phase locking domain does not guarantee perfect phase synchronization for all times. To provide a better understanding of

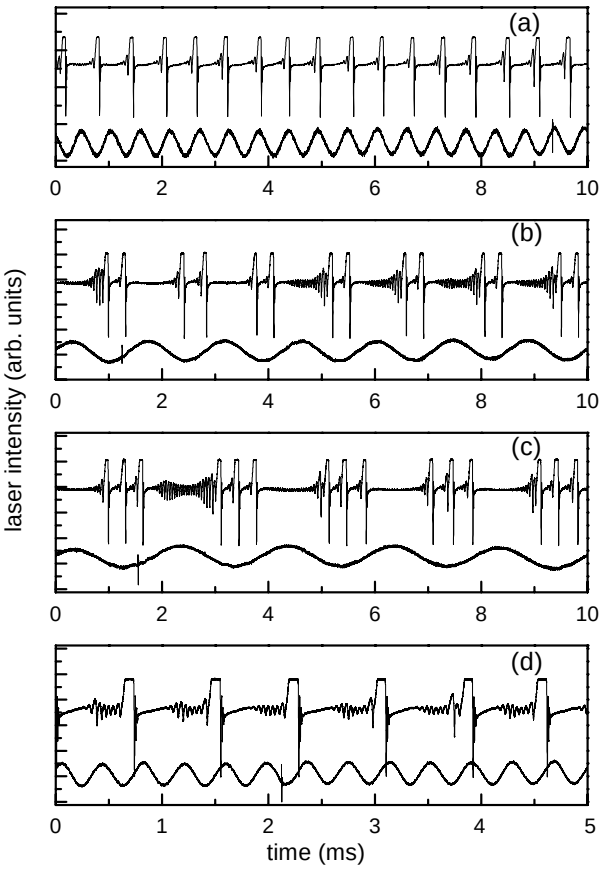

Fig. 3. Experimental time series for different phase synchronizations induced by a frequency modulated control parameter. For comparison, time plots of the modulation control parameter are reported in each case. The modulation frequencies are respectively (a) 1:1 at 1.6 kHz; (b) 1:2 at 0.7 kHz; (c) 1:3 at 0.5 kHz; (d) 2:1 at 2.6 kHz.

phase synchronization in our system, we explore the possible occurrence of phase slips. By this we mean jumps (of multiples of 2π) of the phase difference between the laser output and modulation. The phase of the laser intensity is defined as $\varphi(t) = 2\pi n(t)$, where $n(t)$ is the number of spikes occurring in a time interval t.

In Fig. 5, we report the phase difference between the laser output intensity and the modulation $S(t) = \varphi(t) - 2\pi\nu t$ for different ν's within the synchronization domain corresponding to 1:1 locking. Departing from the perfect synchronization (zero phase slip) and approaching the edges of the domain the slip rate increases. This phenomenon of imperfect phase synchronization has been studied theoretically in the forced Lorenz system [22,23].

Here, we exploit the slip rate information to re-adjust the value of the modulation frequency in order to reach perfect synchronization. Precisely, we introduce the

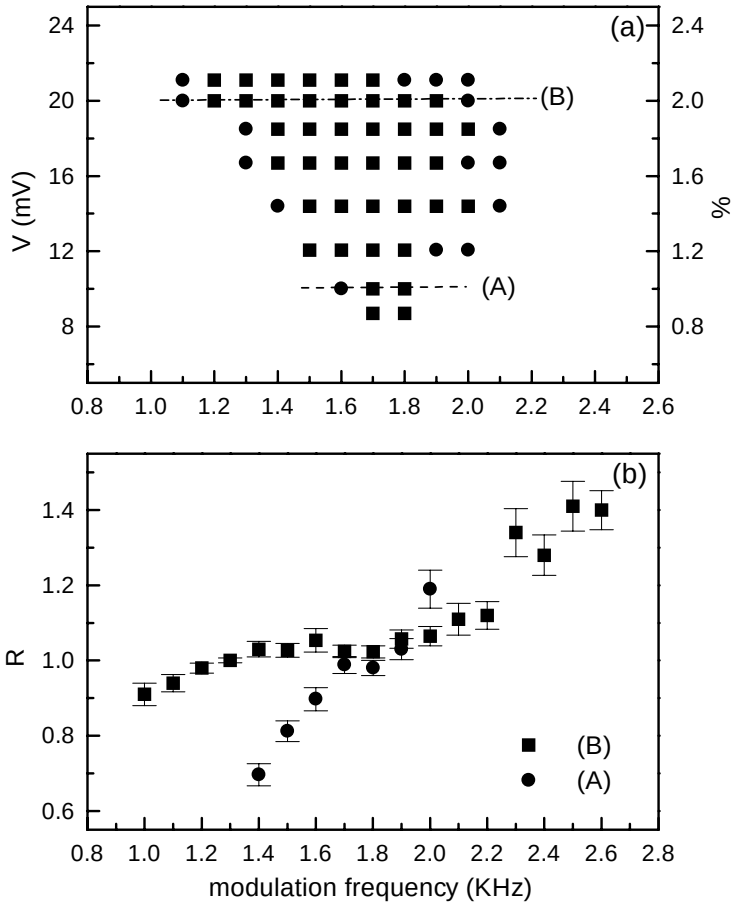

Fig. 4. (a) Phase synchronization domain for the 1:1 locking ratio. Vertical axis: modulation amplitude in mV and %; horizontal axis: modulation frequency in kHz. The domain edge points (black circles) correspond to a phase slip more frequent than any 10 returns. (b) Locking parameter R versus the modulation frequency for the two amplitudes 10 mV (circles) and 20 mV (squares).

average phase slip rate $(\mathrm{d}S/\mathrm{d}t)_{\Delta t}$ defined as the number of jumps S divided by the number Δt of periods of the modulation over which the former number has been evaluated, $(\mathrm{d}S/\mathrm{d}t)_{\Delta t}$ goes to zero at the natural frequency (Fig. 5(a)); otherwise there is a lead or a lag depending on whether the modulation frequency is below or above the natural frequency, respectively. Furthermore, the chaotic character of the slip occurrences is shown by the variance $\langle((\mathrm{d}S/\mathrm{d}t)_{\Delta t} - \langle(\mathrm{d}S/\mathrm{d}t)\rangle)^2\rangle$, where the angular brackets denote an average over very large Δt. The control consists in applying increments $\Delta v = -a(\mathrm{d}S/\mathrm{d}t)_{\Delta t}$ ($a > 0$ being a suitable coefficient) to the modulation frequency at every time increment Δt, so that the modulation frequency as a function of time is given by $v(t) = v_0 + \Sigma\Delta v(t)$, where v_0 is the unperturbed

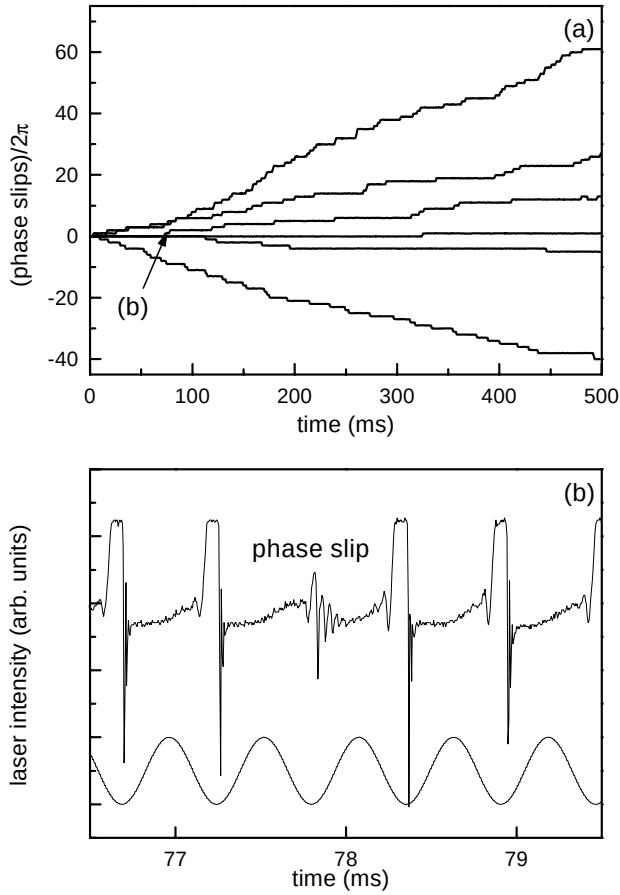

Fig. 5. (a) Phase slips at different frequencies for the 20 mV amplitude (horizontal line B in Fig. 4(a)). The dynamical system monotonically lags or leads in phase depending on whether the modulation frequency is above or below the perfect synchronization (no slips) value of 1.6 kHz. (b) Expanded view of the time in a phase slip. The phase slip is like a defect in a periodic one-dimensional pattern; in fact in this case it is a missed return to the surface of section.

modulation frequency, and the sum being extended over all the intervals Δt up to time t.

In the experiment, we compare the output signal with the modulation signal over a time interval Δt, evaluate the slip rate $(\mathrm{d}S/\mathrm{d}t)_{\Delta t}$ and re-adjust, correspondingly, the frequency of a waveform generator which modulates the laser power supply. If Δt is small, local fluctuations from the average yield a bad control, whereas for large Δt the slip rate has a small variance, thus we expect an asymptotic Δt beyond which the slip rate becomes negligible, as confirmed by the experiment (Fig. 6). Of course, the persistent application of such a control brings the modified modulation frequency asymptotically close to the natural frequency.

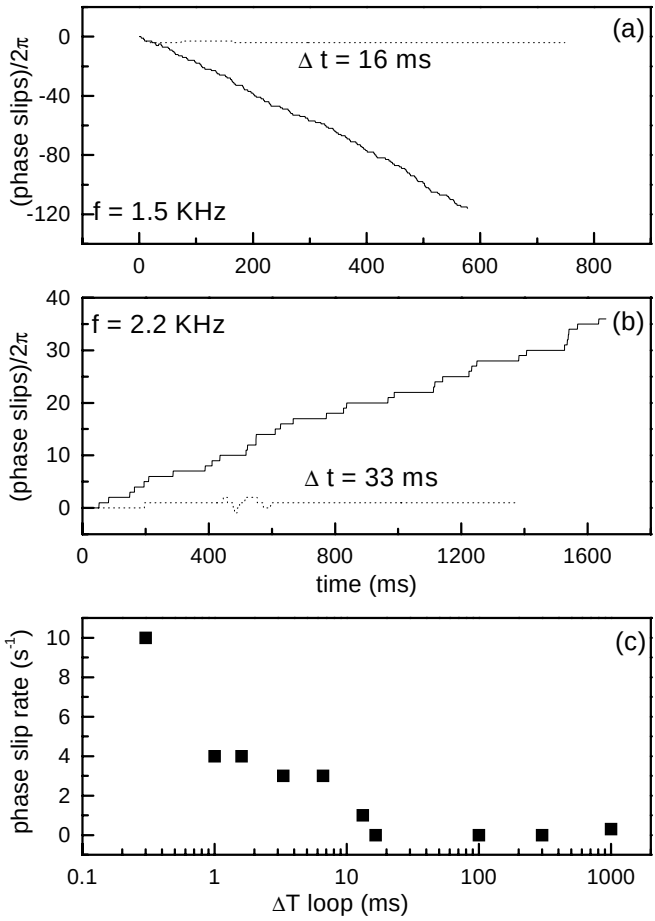

Fig. 6. Long time correction of the phase slip in two cases where the uncontrolled frequency setting of the modulation is below (a) or above (b) the frequency corresponding to the perfect synchronization, solid and dotted lines represent the uncontrolled and controlled case, respectively. (c) Dependence of the residual phase slip upon the sampling time in case (b).

Thus, so far, we have considered a sinusoidal perturbation. If we call "susceptibility" the amount of system response for a unit perturbation, this susceptibility will be maximum around the saddle focus. In fact, the dynamical behavior corresponds to going across the critical point of a second order phase transition at each orbit. This implies not only a critical divergence of the susceptibility around the saddle focus, but also a critical slowing down of the three system coordinates which correspond to the eigenvectors of the saddle focus. Incidentally, this is the reason why we expect that a homoclinic behavior is universal for biological clocks: independent of the number of variables which rule the

activator–inhibitor competition giving rise to a quasi-periodic behavior, only three remain active at the critical point, and all the others are "slaved", to use the language of synergetics [28].

To prove that the susceptibility has a maximum value within the cycle, we have replaced the external modulation by a train of spikes, each one being much shorter than the period. This way, the homoclinic system becomes phase locked to the spike train at saddle focus and not elsewhere, as shown in Fig. 7.

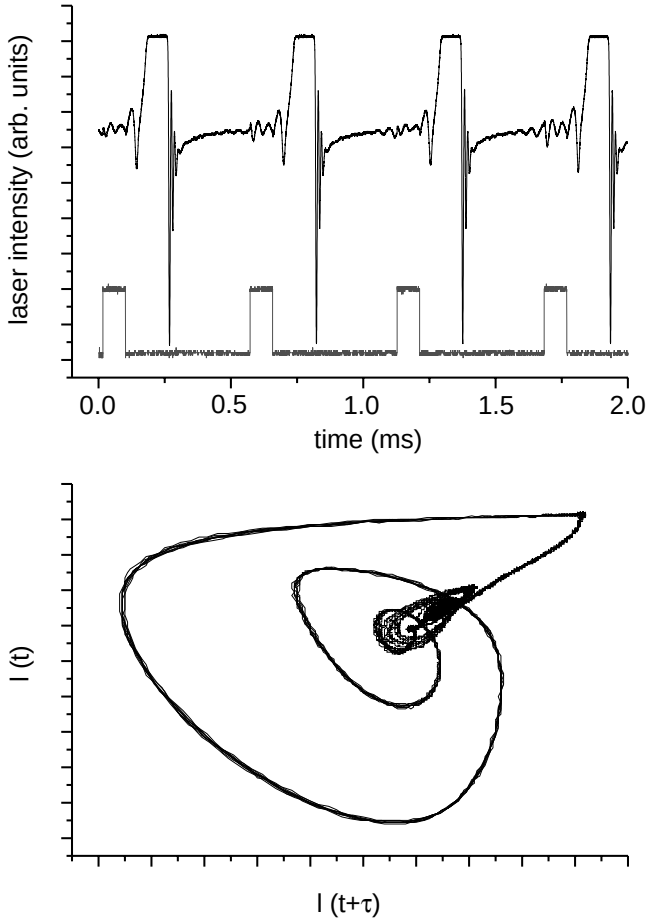

Fig. 7. If the modulation is a periodic train of short spikes rather than a sinusoid, the phase of the homoclinic cycle re-adjusts in order to synchronize the highest susceptibility fraction of the cycle with the perturbing pulse; that fraction coincides with the approximate position of the saddle focus along the orbit.

4. Conclusions

We have shown that homoclinic chaos can be synchronized by use of the temporal information contained in the main spikes. However, the stabilization of a periodic orbit approaching the saddle focus remains difficult to obtain due to the frequent jumps among the many unstable periodic orbits contained in a window of homoclinic chaos. The synchronization of the main spikes is perfect as the modulation frequency matches the average return frequency. As we move away from this condition, we measure an increasing amount of phase slips. This however can be controlled by a secondary feedback loop which acts on the modulation frequency. This result suggests a possible implementation of an adaptive pace maker, which does not impose its own frequency, but re-adjusts its frequency upon the request of the dynamical system. The implications for biological clocks seem very promising. Rather than imposing a pre-set frequency, we can re-adjust the frequency based upon the system needs.

Acknowledgements

We acknowledge partial support from the European Contract No. HPRN-CT-2000-00158. A.D.G. is supported by the European Contract No. PSS 1043.

References

[1] Ott E. Chaos in dynamical systems. Cambridge: Cambridge University Press, 1993.
[2] Hilborn RC. Chaos and nonlinear dynamics. Oxford: Oxford University Press, 1994.
[3] Sil'nikov LP. Sov Math Dokl 1965;6:163.
[4] Arneodo A, Coullet P, Spiegel EA, Tresser C. Physica D 1985;14:327.
[5] Argoul F, Arnéodo A, Richetti P. J Chem Phys 1987;84:1367.
[6] Arecchi FT, Lapucci A, Meucci R, Roversi GA, Coullet PH. Europhys Lett 1988;6:677.
[7] Arecchi FT, Gadomski W, Lapucci A, Mancini H, Meucci R, Roversi GA. J Opt Soc Am B 1988;5:1153.
[8] Pisarchick AN, Meucci R, Arecchi FT. Phys Rev E 2000;62:8823.
[9] Winfree AT. The geometry of biological time. New York: Springer, 1980.
[10] Goldbeter A. Biochemical oscillations and cellular rhythms. Cambridge: Cambridge University Press, 1996.
[11] Keener J, Sneyd J. Mathematical physiology. New York: Springer, 1998.
[12] Keener J, Sneyd J. Nonlinear dynamics of physiological control. Chaos 1991;1(3).
[13] Keener J, Sneyd J. Dynamical disease: mathematical analysis of human illness. Chaos 1995;5(1–4).
[14] Keener J, Sneyd J. Synchronization and patterns in complex systems. Chaos 1996;6(3).
[15] Arecchi FT, Lapucci A, Meucci R. Physica D 1993;62:186.
[16] von der Malsburg C, Schneider W. Biol Cybernet 1986;54:29.
[17] Singer W. Concepts Neurosci 1990;1:1.
[18] Pecora LM, Carroll TL. Phys Rev Lett 1990;64:821.
[19] Rosenblum MG, Pikovsky AS, Kurths J. Phys Rev Lett 1996;76:1804.
[20] Pikovsky AS, Rosenblum MG, Osipov GV, Kurths J. Physica D 1997;104:219.
[21] Pikovsky AS, Zaks MA, Rosenblum MG, Osipov GV, Kurths J. Chaos 1997;7:680.
[22] Zaks MA, Park EH, Rosenblum MG, Kurths J. Phys Rev Lett 1999;82:4228.

[23] Park EH, Zaks MA, Kurths J. Phys Rev Lett C 1999;60:6627.
[24] VanWiggeren GD, Roy R. Science 1998;279:1198.
[25] Schafer C, Rosenblum MG, Kurths J, Abel HH. Nature 1998;392:239.
[26] Neiman A, Pei X, Russel D, Wojtenek W, Wilkens L, Moss F, Braun HA, Huber MT, Voigt K. Phys Rev Lett 1999;82:660.
[27] Allaria E, Arecchi FT, Di Garbo A, Meucci R. Phys Rev Lett 2001;86:791.
[28] Haken H. Synergetics, 3rd ed.. Berlin: Springer, 1983.